View metadata, citation and similar papers at core.ac.uk
brought to you by CORE
provided by Elsevier - Publisher Connector

International Journal of Solids and Structures 51 (2014) 2073–2083

Contents lists available at ScienceDirect

International Journal of Solids and Structures

journal homepage: www.elsevier.com/locate/ijsolstr

An equivalent classical plate model of corrugated structures

Zheng Ye [a], Victor L. Berdichevsky [b], Wenbin Yu [c,*]

[a] Utah State University, Logan, Utah 84322, United States
[b] Wayne State University, Detroit, Michigan 48202, United States
[c] Purdue University, West Lafayette, Indiana 47907-2045, United States

ARTICLE INFO

Article history:
Received 25 June 2013
Received in revised form 12 February 2014
Available online 1 March 2014

Keywords:
Corrugated structure
Plate
Variational asymptotic method

ABSTRACT

An equivalent classical plate model of corrugated structures is derived using the variational asymptotic method. Starting from a thin shell theory, we carry out an asymptotic analysis of the strain energy in terms of the smallness of a single corrugation with respect to the characteristic length of macroscopic deformation of the corrugated structure. We obtained the complete set of analytical formulas for effective plate stiffnesses valid for both shallow and deep corrugations. These formulas can reproduce the well-known classical plate stiffnesses when the corrugated structure is degenerated to a flat plate. The extension–bending coupling stiffnesses are obtained the first time. The complete set of relations are also derived for recovering the local fields of corrugated structures.

© 2014 Elsevier Ltd. All rights reserved.

1. Introduction

Corrugated structures have been widely used in civil, automotive, naval and aerospace engineering, to name only some, diaphragms for sensing elements, fiberboards, folded roofs, container walls, sandwich plate cores, bridge decks, ship panels, etc. (Andreeva, 1966; Mccready and Katz, 1939; Seaquist, 1964; Baum et al., 1981; Carlsson et al., 2001; Liang et al., 2001; Davalos et al., 2001; Buannic et al., 2003; Aboura et al., 2004; Talbi et al., 2009; Haj-Ali et al., 2009; Viguié et al., 2011). Recently, corrugated structures are also applied for flexible wings or morphing wings (Yokozeki et al., 2006; Gentilinia et al., 2009; Thill et al., 2010) due to their unique characteristics of having orders of magnitude different stiffnesses in different directions.

Although commercial codes allow one to analyze corrugated structures by meshing all the corrugations using shell elements or solid elements, it is not a practical way to finish prototype in a timely manner as it requires significant computing time, particularly if the structure is formed by hundreds or thousands of corrugations. The common practice in analysis of corrugated structures is to model it as an equivalent flat plate, which is possible if the period of corrugation is much smaller than the characteristic length of macroscopic deformation of the structure (see Fig. 1). For example, to model the corrugated structure using the Kirchhoff plate model, also called the classical plate model, we need to obtain the following strain energy by analyzing a single corrugation:

$$J=\frac{1}{2}\begin{Bmatrix}\epsilon_{xx}\\ \epsilon_{yy}\\ 2\epsilon_{xy}\\ \kappa_{xx}\\ \kappa_{yy}\\ 2\kappa_{xy}\end{Bmatrix}^T\begin{Bmatrix}A_{11} & A_{12} & 0 & B_{11} & B_{12} & 0\\ A_{12} & A_{22} & 0 & B_{12} & B_{22} & 0\\ 0 & 0 & A_{66} & 0 & 0 & B_{66}\\ B_{11} & B_{12} & 0 & D_{11} & D_{12} & 0\\ B_{12} & B_{22} & 0 & D_{12} & D_{22} & 0\\ 0 & 0 & B_{66} & 0 & 0 & D_{66}\end{Bmatrix}\begin{Bmatrix}\epsilon_{xx}\\ \epsilon_{yy}\\ 2\epsilon_{xy}\\ \kappa_{xx}\\ \kappa_{yy}\\ 2\kappa_{xy}\end{Bmatrix} \quad (1)$$

where x, y are the two in-plane coordinates describing the equivalent plate, $\epsilon_{xx}, \epsilon_{yy}, \epsilon_{xy}$ the membrane strains, $\kappa_{xx}, \kappa_{yy}, \kappa_{xy}$ the curvature strains, A_{ij}, D_{ij} and B_{ij} represent extension stiffnesses, bending stiffnesses, and extension–bending couplings, respectively. The stiffness matrix in Eq. (1) could be in general populated for an equivalent plate model of general corrugated structures. However, it will be shown later that some of the stiffness constants vanish as shown in Eq. (1) for a corrugated structure made of a single isotropic material.

The literature is rich in equivalent plate modeling of corrugated structures with the first treatment known to the authors dated 1923 (Huber, 1923) and a very recent treatment appeared in 2013 (Bartolozzi et al., 2013). Various methods with different levels of sophistication were used in numerous studies. Generally speaking, existing methods can be generally classified either as engineering approaches based on various assumptions or asymptotic approaches based on asymptotic analysis of governing differential equations of a shell theory. Most methods fall in the category of engineering approaches which invoke various assumptions for boundary conditions and force/moment distribution within the corrugated structure. For a given state of constant strain, the actual

* Corresponding author. Tel.: +1 7644945142.
E-mail address: wenbinyu@purdue.edu (W. Yu).

http://dx.doi.org/10.1016/j.ijsolstr.2014.02.025
0020-7683/© 2014 Elsevier Ltd. All rights reserved.

(or assumed) distributions of forces and moments within the corrugated structure will be determined. Then force or energy equivalence is used to derive the corresponding stiffness constants (see Briassoulis, 1986; Xia et al., 2012; Bartolozzi et al., 2013 and references cited therein). Although both analytical approach and finite element analysis can be used to predict these stiffness constants, the analytical approach has the advantage of providing a set of close-form expressions in terms of the material and geometry characteristics of the corrugated structure while the finite element analysis predicts values which are valid for a specific corrugated structure. Asymptotic approaches exploit the smallness of a single corrugation with respect to characteristic length of macroscopic deformation of the corrugated structure (Andrianov et al., 1998; Manevich et al., 2002; Arkhangelskii and Gorbachev, 2007; Andrianov et al., 2009). Substituting asymptotic expansion of the field variables into the governing differential equation of the shell theory, a series of system of governing differential equations corresponding to different orders can be solved to find the relationship between the equivalent plate and the corrugated structure. Because different methods are used to treat this problem, it is not surprising that different results are obtained in previous studies, which will summarized and compared here.

2. Results

To facilitate the comparison of different results in the literature, we need to set up the necessary notations. Let x be the Cartesian coordinate in the corrugation direction and ε the projected length of the corrugation Fig. 2. We denote by $X = \frac{x}{\varepsilon}$, the dimensionless "cell coordinate". Within a cell, X changes between $-1/2$ and $1/2$. For any parameter, f, changing within a cell, $\langle f \rangle \equiv \int_{-\frac{1}{2}}^{\frac{1}{2}} f(X)dX$. The shape of the corrugation is described by the $x_3(X)$ which is a periodic function with the period unity. Without loss of generality, one can set

$$\langle x_3 \rangle = 0, \tag{2}$$

by shifting the observer's frame in the vertical direction. Let us also denote

$$x_3 = \varepsilon\phi(X), \quad \varphi = \frac{dx_3(x)}{dx} = \frac{d\phi(X)}{dX}, \quad a = 1 + \varphi^2, \tag{3}$$

we can compute the arc-length of the corrugation S and the moment of inertia along the corrugation direction I_y as

$$S = \varepsilon\langle\sqrt{a}\rangle, \quad I_y = h\varepsilon^2\langle\phi^2\sqrt{a}\rangle. \tag{4}$$

2.1. Results from previous studies

Seydel (1931) followed Huber (1923) and obtained the following formulas for the equivalent bending stiffnesses

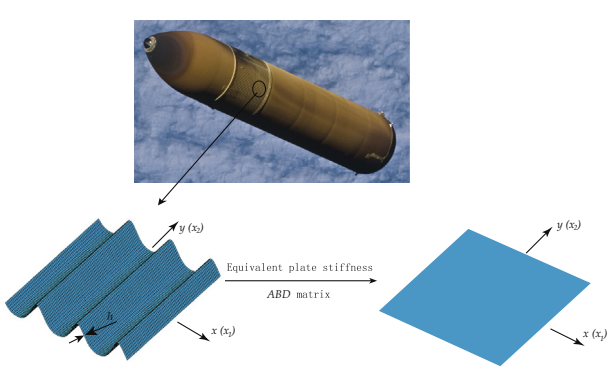

Fig. 1. Equivalent plate modeling of corrugated structures.

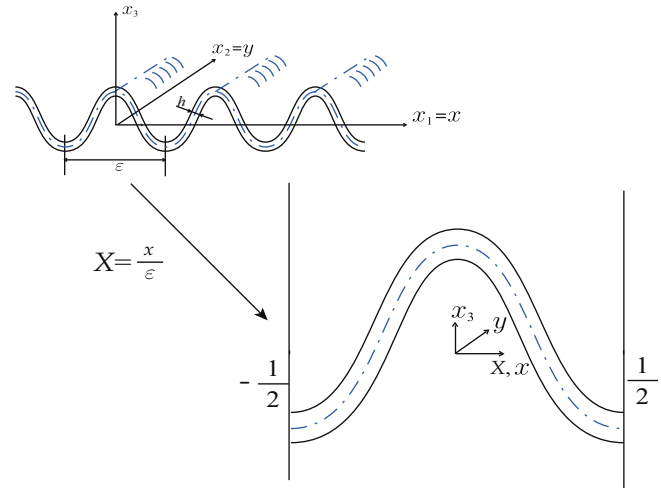

Fig. 2. Shell geometry and unit cell.

$$D_{11} = \frac{\varepsilon}{S}\frac{Eh^3}{12(1-\nu^2)}, \quad D_{12} = 0, \quad D_{22} = EI_y, \quad D_{66} = \frac{S}{\varepsilon}\frac{Eh^3}{24(1+\nu)}. \tag{5}$$

Here h denotes the thickness Fig. 3. It is assumed that the corrugated plate is made of isotropic elastic material with the Young's modulus E, and the Poisson's ratio ν. These results are also widely cited in textbooks (Szilard, 1974; Bending et al., 1976; McFarland et al., 1972). In later works, approximations for S and I_y for different corrugated shapes were obtained (Lekhnitskii, 1968; Szilard, 1974; Lau, 1981; Lee, 1981). A review of different approximate formulas of S and I_y for various corrugation shapes can be found in Luo et al. (1992). This is not needed as it is easy to evaluate the two integrals in Eq. (4) accurately for any given corrugated shape using computers nowadays.

Later, Briassoulis (1986) proposed the following modified relations

$$D_{11} = \frac{\varepsilon}{S}\frac{Eh^3}{12(1-\nu^2)}, \quad D_{12} = \nu D_{11},$$
$$D_{22} = \frac{EhT^2}{2} + \frac{Eh^3}{12(1-\nu^2)}, \quad D_{66} = \frac{Eh^3}{24(1+\nu)}. \tag{6}$$

Here T is the rise of the corrugations measured to middle surface as shown in Fig. 3. Briassoulis correctly recognized D_{12} due to the Poisson's effect. However, as will be shown later, the formulas for D_{22} and D_{66} are not correct. The expression for D_{22} is obtained by assuming a sinusoidal corrugated profile, $x_3 = T\sin(2\pi x/\varepsilon)$. Briassoulis's relations are also used in Liew et al. (2006, 2009) and

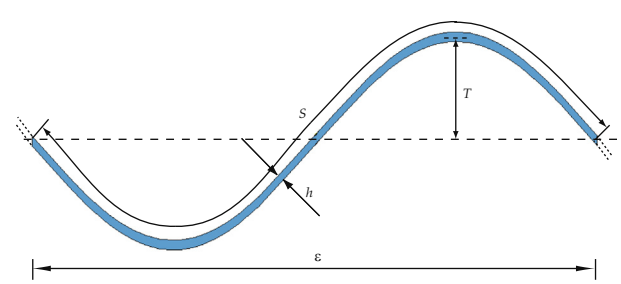

Fig. 3. Unit cell of a corrugated structure (sinusoidal shape is used for illustration).

Wennberg et al. (2011) with D_{22} modified in Liew et al. (2006) for a trapezoidal corrugated profile.

Recently, Xia et al. (2012) obtained the following formulas for bending stiffnesses

$$D_{11} = \frac{\varepsilon}{S}\frac{Eh^3}{12(1-\nu^2)}, \quad D_{12} = \nu D_{11},$$
$$D_{22} = \frac{EI_y}{1-\nu^2} + \left\langle \frac{1}{\sqrt{a}} \right\rangle \frac{Eh^3}{12(1-\nu^2)}, \quad D_{66} = \frac{S}{\varepsilon}\frac{Eh^3}{24(1+\nu)}. \tag{7}$$

There are other bending stiffnesses proposed in the literature such as those cited by Samanta et al. (1999) from Easley et al. (1969) and Easley (1975) which are not listed here because they are not as complete and accurate as those listed here.

The equivalent extension stiffnesses were originally found for applications such as roofs and shear walls in 1960–70s (El-Atrouzy, 1969; Abdel-Sayed, 1970; Marzouk et al., 1973; Davies, 1976; El-Atrouzy and Abdel-Sayed, 1978; Easley, 1975). The commonly accepted formulas in literature are:

$$A_{11} = \frac{Eh^3}{6(1-\nu^2)T^2}, \quad A_{12} = \nu A_{11}, \quad A_{22} = \frac{S}{\varepsilon}Eh, \quad A_{66} = \frac{\varepsilon}{S}\frac{Eh}{2(1+\nu)}. \tag{8}$$

Later, in Briassoulis (1986), Briassoulis provided different formulas for A_{11} and A_{66}

$$A_{11} = \frac{Eh^3}{h^2 + 6(1-\nu^2)T^2\left(\frac{S^2}{\varepsilon^2} - \frac{S}{2\pi\varepsilon}\sin\frac{2\pi S}{\varepsilon}\right)}, \quad A_{66} = \frac{Eh}{2(1+\nu)}. \tag{9}$$

with $A_{12} = \nu A_{11}$ and A_{22} the same as that in Eq. (8). Again, the expression for A_{11} is obtained by assuming a sinusoidal corrugated profile, $x_3 = T\sin(2\pi x/\varepsilon)$.

Recently, Xia et al. (2012) obtained the following formulas for extension stiffnesses

$$A_{11} = \frac{Eh^3}{12(1-\nu^2)}\frac{1}{\left\langle\frac{1}{\sqrt{a}}\right\rangle\frac{h^2}{12} + \frac{I_y}{h}}, \quad A_{12} = \nu A_{11},$$
$$A_{22} = \nu^2 A_{11} + \frac{S}{\varepsilon}Eh\left(\frac{1}{1-\nu^2} - \frac{1-\nu^2}{4(1+\nu)^2}\right), \quad A_{66} = \frac{\varepsilon}{S}\frac{Eh}{2(1+\nu)}. \tag{10}$$

Andrianov et al. (1998, 2009), Manevich et al. (2002) and Arkhangelskii and Gorbachev (2007) obtained different equations by asymptotic analysis of elasticity equations, but the origin of deviations remains unclear.

2.2. Present results

We obtained the following general relations for the equivalent plate stiffnesses for corrugated structures:

$$A_{11} = \frac{E}{1-\nu^2}\frac{12\varepsilon^2\langle\varphi\mathcal{A}\rangle}{h\mathcal{C}^2} + \frac{Eh}{1-\nu^2}\left\langle\frac{1}{\sqrt{a}}\right\rangle\frac{1}{\mathcal{C}^2}, \quad A_{12} = \nu A_{11},$$
$$A_{22} = Eh\langle\sqrt{a}\rangle + \nu^2 A_{11}, \quad A_{66} = \mu h\alpha_1,$$
$$B_{11} = \frac{E}{1-\nu^2}\frac{12\varepsilon^3\langle\varphi\mathcal{A}\rangle}{h\mathcal{C}^2}\mathcal{B} + \frac{Eh}{1-\nu^2}\left\langle\frac{1}{\sqrt{a}}\right\rangle\frac{1}{\mathcal{C}^2}\mathcal{B}\varepsilon, \quad B_{12} = \nu B_{11},$$
$$B_{22} = Eh\varepsilon\langle\sqrt{a}\phi\rangle + \nu^2 B_{11}, \quad B_{66} = \mu h\alpha_2,$$
$$D_{11} = \frac{Eh^3}{12(1-\nu^2)}\left(\frac{12^2\varepsilon^4\mathcal{B}^2}{h^4\mathcal{C}^2}\langle\varphi\mathcal{A}\rangle + \frac{1}{\langle\sqrt{a}\rangle}\right) + \frac{Eh}{1-\nu^2}\frac{\varepsilon^2\mathcal{B}^2}{\mathcal{C}^2}\left\langle\frac{1}{\sqrt{a}}\right\rangle,$$
$$D_{22} = Eh\varepsilon^2\langle\phi^2\sqrt{a}\rangle + \frac{Eh^3}{12}\left\langle\frac{1}{\sqrt{a}}\right\rangle + \nu^2 D_{11}, \quad D_{12} = \nu D_{11},$$
$$D_{66} = \frac{\mu h}{4}\left\langle\frac{\sqrt{a}}{3}h^2 - \frac{1}{\sqrt{a}}\frac{\frac{h^4\varphi'^2}{12^2\varepsilon^2 a^2} - a\alpha_2^2}{1+\frac{\varphi'^2h^2}{48\varepsilon^2a^3}}\right\rangle. \tag{11}$$

where

$$\mathcal{B} = \frac{\langle\sqrt{a}\phi\rangle}{\langle\sqrt{a}\rangle}, \quad \mathcal{C} = -12\langle\varphi\mathcal{A}\rangle\frac{\varepsilon^2}{h^2} - \left\langle\frac{1}{\sqrt{a}}\right\rangle, \quad \alpha_1 = 1\Bigg/\left\langle\frac{\sqrt{a}}{1+\frac{\varphi'^2h^2}{48\varepsilon^2a^3}}\right\rangle,$$
$$\alpha_2 = \alpha_1\left\langle\frac{\frac{h^2\varphi'}{12\varepsilon a}}{1+\frac{\varphi'^2h^2}{48\varepsilon^2a^3}}\right\rangle, \tag{12}$$

and

$$\mathcal{A}(X) = -\int_0^X\sqrt{a}\phi(Y)dY + \mathcal{B}\int_0^X\sqrt{a}dY \tag{13}$$

We also obtained the following relations for recovering the shell strains in the original corrugated structure:

$$\gamma_{11}^0 = c_1\sqrt{a} - \nu a(\epsilon_{yy} + x_3\kappa_{yy}), \quad 2\gamma_{12}^0 = \frac{\sqrt{a}c_2 - \frac{h^2\varphi'\kappa_{xy}}{12\varepsilon a}}{1+\frac{\varphi'^2h^2}{48\varepsilon^2a^3}},$$
$$\gamma_{22}^0 = \epsilon_{yy} + x_3\kappa_{yy}, \quad \rho_{11}^0 = a\left(c_1\frac{12x_3}{h^2} + c_4\right) + \nu\sqrt{a}\kappa_{yy},$$
$$2\rho_{12}^0 = -\frac{2\sqrt{a}\kappa_{xy} + \frac{\varphi'}{2\varepsilon a}c_2}{1+\frac{\varphi'^2h^2}{48\varepsilon^2a^3}}, \quad \rho_{22}^0 = -\frac{1}{\sqrt{a}}\kappa_{yy}. \tag{14}$$

with

$$c_1 = \frac{\varepsilon\mathcal{B}(v_{3,11} + \nu v_{3,22}) - (v_{1,1} + \nu v_{2,2})}{\mathcal{C}}, \tag{15}$$
$$c_2 = \alpha_1(v_{1,2} + v_{2,1}) - \alpha_2 v_{3,12}, \tag{16}$$
$$c_4 = \frac{1}{\langle\sqrt{a}\rangle}(v_{3,11} + \nu v_{3,22}) - \frac{12}{h^2}c_1\frac{\langle x_3\sqrt{a}\rangle}{\langle\sqrt{a}\rangle}. \tag{17}$$

In general, the coupling stiffnesses, B_{ij}, contrary to what has been commonly assumed the literature, are not zero. They vanish, however, for symmetric corrugations of which $\phi(X)$ is an odd function of X.

$$-\phi(X) = \phi(-X), \tag{18}$$

and due to periodicity of $\phi(X)$, $\phi(1/2) = 0$. Derivative $\varphi = d\phi/dX$ is an even function, and so is $a = 1 + \varphi^2$. Therefore, $\phi\sqrt{a}$ is an odd function, $\langle\phi\sqrt{a}\rangle = 0$. Thus $\mathcal{B} = 0$. Derivative φ' is an odd function thus $\alpha_2 = 0$. The equivalent plate stiffnesses can be simplified for a symmetric corrugation as

$$A_{11} = \frac{E}{1-\nu^2}\frac{12\varepsilon^2\langle\varphi\mathcal{A}\rangle}{h\mathcal{C}^2} + \frac{Eh}{1-\nu^2}\left\langle\frac{1}{\sqrt{a}}\right\rangle\frac{1}{\mathcal{C}^2}, \quad A_{12} = \nu A_{11},$$
$$A_{22} = Eh\langle\sqrt{a}\rangle + \nu^2 A_{11}, \quad A_{66} = \mu h\alpha_1, \quad B_{11} = B_{12} = B_{22} = B_{66} = 0,$$
$$D_{11} = \frac{Eh^3}{12(1-\nu^2)}\frac{1}{\langle\sqrt{a}\rangle}, \quad D_{22} = Eh\varepsilon^2\langle\phi^2\sqrt{a}\rangle + \frac{Eh^3}{12}\left\langle\frac{1}{\sqrt{a}}\right\rangle + \nu^2 D_{11},$$
$$D_{12} = \nu D_{11}, \quad D_{66} = \frac{\mu h}{4}\left\langle\frac{\sqrt{a}}{3}h^2 - \frac{1}{\sqrt{a}}\frac{\frac{h^4\varphi'^2}{12^2\varepsilon^2a^2}}{1+\frac{\varphi'^2h^2}{48\varepsilon^2a^3}}\right\rangle. \tag{19}$$

The formulas for c_1, c_2, c_4 needed for recovery relations in Eq. (14) can also be simplified for a symmetric corrugation.

$$c_1 = -\frac{(v_{1,1} + \nu v_{2,2})}{\mathcal{C}}, \quad c_2 = \alpha_1(v_{1,2} + v_{2,1}), \quad c_4 = \frac{(v_{3,11} + \nu v_{3,22})}{\langle\sqrt{a}\rangle}. \tag{20}$$

2.3. Discussion of the results

First, we perform a simple consistence check for all the results. For equivalent plate stiffnesses to be valid for general corrugated structures, they should be able to reproduce the well-known classical plate stiffnesses when the corrugated structure degenerated to be a flat plate, for which we have

$$\varphi = \phi = \mathcal{A} = \mathcal{B} = 0, \quad \sqrt{a} = 1, \quad \mathcal{C} = -1, \quad \alpha_1 = 1, \quad \alpha_2 = 0. \tag{21}$$

The expressions in Eq. (11) are indeed simplified to be the well known stiffness formulas for the classical model of isotropic homogeneous plates.

The bending stiffnesses in Eq. (5) cannot reproduce the case of a flat plate while those in Eqs. (6) and (7) can. However, none of the extension stiffness from previous studies can reproduce the case of a flat plate.

For shallow corrugation, we know $\phi \sim \delta \ll 1$ and no specific order can be said regarding the magnitude of $\frac{h}{\varepsilon}$. We can use this small parameter to simplify our formulas. We have

$$\mathcal{B} \sim \delta, \quad \mathcal{C} = -\left\langle \frac{1}{\sqrt{a}} \right\rangle, \quad \alpha_1 = \frac{1}{\langle \sqrt{a} \rangle}, \quad \alpha_2 = \alpha_1 \left\langle \frac{h^2 \varphi'}{12\varepsilon a} \right\rangle \sim \delta. \tag{22}$$

The leading terms of the equivalent plate stiffness are

$$A_{11} = \frac{Eh}{1-\nu^2} \frac{1}{\left\langle \frac{1}{\sqrt{a}} \right\rangle}, \quad A_{12} = \nu A_{11}, \quad A_{22} = Eh\langle \sqrt{a} \rangle + \nu^2 A_{11},$$

$$A_{66} = \frac{\mu h}{\langle \sqrt{a} \rangle}, \quad B_{11} = \frac{Eh}{1-\nu^2} \frac{1}{\left\langle \frac{1}{\sqrt{a}} \right\rangle} \mathcal{B}\varepsilon, \quad B_{12} = \nu B_{11},$$

$$B_{22} = Eh\varepsilon \langle \sqrt{a}\phi \rangle + \nu^2 B_{11}, \quad B_{66} = \mu h \alpha_2, \quad D_{11} = \frac{Eh^3}{12(1-\nu^2)} \frac{1}{\langle \sqrt{a} \rangle},$$

$$D_{12} = \nu D_{11} \quad D_{22} = \frac{Eh^3}{12} \left\langle \frac{1}{\sqrt{a}} \right\rangle + \nu^2 D_{11}, \quad D_{66} = \frac{\mu h^2}{12} \langle \sqrt{a} \rangle. \tag{23}$$

Note B_{ij} vanish for symmetric corrugations. The above formulas can degenerate to those for a flat plate. Comparing to the results from previous studies, we can see that Seydel's formulas (Seydel, 1931) for D_{11} and D_{66} in Eq. (5) can be used for shallow corrugations. However D_{12} and D_{22} are not valid for shallow corrugations. Briassoulis' formulas (Briassoulis, 1986) for D_{11} and D_{12} in Eq. (6) are valid for shallow corrugations but D_{22} and D_{66} are not valid. The formulas of Xia et al. (2012) in Eq. (7) can be used for shallow corrugations except D_{22}.

For most corrugated structures, we have $h/\varepsilon \ll 1$. This small parameter can be used to simplify our formulas. We have

$$\mathcal{C} \approx -12\langle \varphi \mathcal{A} \rangle \frac{\varepsilon^2}{h^2}, \quad \alpha_1 \approx \frac{1}{\langle \sqrt{a} \rangle} \tag{24}$$

The leading terms of equivalent plate stiffnesses become:

$$A_{11} = \frac{Eh^3}{12(1-\nu^2)\varepsilon^2 \langle \varphi \mathcal{A} \rangle}, \quad A_{12} = \nu A_{11}, \quad A_{22} = Eh\langle \sqrt{a} \rangle,$$

$$A_{66} = \frac{\mu h}{\langle \sqrt{a} \rangle}, \quad B_{11} = \frac{Eh^3 \mathcal{B}}{12(1-\nu^2)\varepsilon \langle \varphi \mathcal{A} \rangle}, \quad B_{12} = \nu B_{11},$$

$$B_{22} = Eh\varepsilon \langle \phi \sqrt{a} \rangle, \quad B_{66} = \frac{\mu h^3}{12\varepsilon} \frac{\left\langle \frac{\varphi'}{a} \right\rangle}{\langle \sqrt{a} \rangle},$$

$$D_{11} = \frac{Eh^3}{12(1-\nu^2)} \left(\frac{\mathcal{B}^2}{\langle \varphi \mathcal{A} \rangle} + \frac{1}{\langle \sqrt{a} \rangle} \right), \quad D_{12} = \nu D_{11},$$

$$D_{22} = Eh\varepsilon^2 \langle \phi^2 \sqrt{a} \rangle, \quad D_{66} = \frac{\mu h^3}{12} \langle \sqrt{a} \rangle. \tag{25}$$

As follows from Eq. (25), among the extension stiffnesses the largest ones are A_{22} and A_{66}, while A_{11} and A_{12} contain small factor $(h/\varepsilon)^2$:

$$A_{11} \sim A_{12} \sim \left(\frac{h}{\varepsilon}\right)^2 A_{22} \sim \left(\frac{h}{\varepsilon}\right)^2 A_{66}. \tag{26}$$

This corresponds to softness of the corrugated plate in the direction of corrugation. Similarly, for bending stiffnesses, the largest stiffness is D_{22}, and

$$D_{11} \sim D_{12} \sim \left(\frac{h}{\varepsilon}\right)^2 D_{22} \sim D_{66}. \tag{27}$$

Among the coupling stiffnesses the largest one is B_{22}, while

$$B_{11} \sim B_{12} \sim \left(\frac{h}{\varepsilon}\right)^2 B_{22} \sim B_{66}. \tag{28}$$

The equivalent plate stiffness for symmetric corrugations have the form:

$$A_{11} = \frac{Eh^3}{12(1-\nu^2)\varepsilon^2 \langle \phi^2 \sqrt{a} \rangle}, \quad A_{12} = \nu A_{11}, \quad A_{22} = Eh\langle \sqrt{a} \rangle,$$

$$A_{66} = \frac{\mu h}{\langle \sqrt{a} \rangle}, \quad D_{11} = \frac{Eh^3}{12(1-\nu^2)\langle \sqrt{a} \rangle}, \quad D_{12} = \nu D_{11},$$

$$D_{22} = Eh\varepsilon^2 \langle \phi^2 \sqrt{a} \rangle, \quad D_{66} = \frac{\mu h^3}{12} \langle \sqrt{a} \rangle. \tag{29}$$

Comparing to the results from previous studies, we can see that (Seydel, 1931) obtained the correct bending stiffnesses except D_{12} in Eq. (5), (Briassoulis, 1986) obtained the correct bending stiffnesses except D_{22} and D_{66} in Eq. (6). Xia et al. (2012) obtained the correct bending stiffnesses except D_{22} in Eq. (7).

As far as extension stiffnesses are concerned, the commonly accepted formulas in 1960–70s, Eq. (8), are correct if T^2 is defined as half of the average of x_3^2 over the corrugated profile, i.e. $T^2 = \frac{\langle x_3^2 \sqrt{a} \rangle}{2}$. The modified extension stiffnesses in Eq. (9) by Briassoulis (1986) are in fact wrong. The first three formulas of the extension stiffnesses by Xia et al. (2012) in Eq. (10) are correct if higher order term in A_{11} is neglected. A_{22} is approximately correct as the term $\frac{1}{1-\nu^2} - \frac{1-\nu^2}{4(1+\nu)^2}$ is very close to unity for normal materials.

Most of the previous studies focused on obtained the equivalent plate stiffnesses without paying attention to the local stress/strain field within the original corrugated structure, expect Briassoulis attempted to recover the local stress based on the forces and moments obtained from the equivalent plate analysis in Briassoulis (1986). Such relations are derived based on an assumed sinusoidal corrugated profile. However, as we have already shown that half of the equivalent plate bending and extension stiffnesses from Briassoulis (1986) are not correct. The accuracy of the recovery relations can only become worse. Hence, Briassoulis' recovery relations are not listed here and compared with ours.

3. Shell formulation of corrugated structures

Thin-walled corrugated structures can be effectively described by the classical shell theory if the thickness is small compared to the minimum curvature radius, which is of the order of the corrugation period. We choose a Cartesian coordinate system x_i with basic vectors $\hat{\mathbf{e}}_i$. Throughout the paper, Latin indices run through the values 1, 2, and 3; Greek indices assume values 1 and 2, and summation is conducted over repeated indices except where explicitly indicated. The position vector of the shell mid-surface can be considered as a function of coordinates x_1 and x_2:

$$\mathbf{r}(x_1, x_2) = x_1 \hat{\mathbf{e}}_1 + x_2 \hat{\mathbf{e}}_2 + x_3 \hat{\mathbf{e}}_3. \tag{30}$$

If there are corrugations along both x and y directions, x_3 is a function of both coordinates x_1 and x_2. Herein, we restrict our consideration to the case of periodic corrugations in one direction, x, as in Fig. 2. The tangent vectors $\mathbf{a}_\alpha$ of the shell surface can be obtained by differentiating the position vector with respect to x_α, $\mathbf{a}_\alpha = \partial \mathbf{r}/\partial x_\alpha$, so that

$$\mathbf{a}_1 = \hat{\mathbf{e}}_1 + \varphi(x)\hat{\mathbf{e}}_3, \quad \mathbf{a}_2 = \hat{\mathbf{e}}_2, \tag{31}$$

For brevity uses, we also write $\mathbf{a}_\alpha = r^i_\alpha \hat{\mathbf{e}}_i$, which implies

$$r^1_1 = 1, \quad r^2_1 = 0, \quad r^3_1 = \varphi(x), \quad r^1_2 = 0, \quad r^2_2 = 1, \quad r^3_2 = 0. \tag{32}$$

The metric tensor of the shell surface, $a_{\alpha\beta}$, is defined as

$$a_{\alpha\beta} = \mathbf{a}_\alpha \cdot \mathbf{a}_\beta \tag{33}$$

The contravariant components of the surface metric tensor $a^{\alpha\beta}$ are defined according to $a^{\alpha\beta}a_{\gamma\beta} = \delta_{\alpha\gamma}, \delta_{\alpha\gamma}$ being the two-dimensional Kronecker symbol.

The normal vector of the shell mid-surface is:

$$\hat{\mathbf{n}} = \frac{\mathbf{a}_1 \times \mathbf{a}_2}{|\mathbf{a}_1 \times \mathbf{a}_2|} = \frac{-\varphi}{\sqrt{a}}\hat{\mathbf{e}}_1 + \frac{1}{\sqrt{a}}\hat{\mathbf{e}}_3, \tag{34}$$

The second quadratic form of the shell mid-surface is defined as

$$b_{\alpha\beta} = \frac{\partial \mathbf{a}_\alpha}{\partial x_\beta} \cdot \hat{\mathbf{n}}. \tag{35}$$

Hence, we have

$$b_{11} = \frac{1}{\sqrt{a}}\frac{d\varphi}{dx}, \quad b_{12} = b_{22} = 0, \quad b^1_1 = \frac{1}{a^{3/2}}\frac{d\varphi}{dx}, \quad b^2_1 = b^1_2 = b^2_2 = 0, \tag{36}$$

where $b^\alpha_\beta = a^{\alpha\gamma}b_{\gamma\beta}$.

The Christoffel symbols can be found from the equation:

$$\Gamma^\gamma_{\alpha\beta} = \frac{1}{2}a^{\gamma\delta}\left(\frac{\partial a_{\alpha\delta}}{\partial x_\beta} + \frac{\partial a_{\beta\delta}}{\partial x_\alpha} - \frac{\partial a_{\alpha\beta}}{\partial x_\delta}\right). \tag{37}$$

Using Eq. (33), we obtain that all components of $\Gamma^\gamma_{\alpha\beta}$ vanish except

$$\Gamma^1_{11} = \frac{1}{2a}\frac{da}{dx} = \frac{1}{2}\frac{d\ln a}{dx} \tag{38}$$

According to the general theory of periodic structures (Bakhvalov, 1974; Bakhvalov and Panasenko, 1989) (see also Berdichevsky, 2009 chapter 17), the functions describing the behavior of the shell should be considered as functions of the cell coordinate X, and slow coordinates x, and y. All the geometric characteristics we just introduced are functions of X only, e.g.

$$x_3 = \varepsilon\phi(X), \quad \varphi(X) = \frac{d\phi(X)}{dX}, \quad b_{11} = \frac{1}{\varepsilon\sqrt{a}}\frac{d\varphi}{dX},$$
$$b^1_1 = \frac{1}{\varepsilon a^{3/2}}\frac{d\varphi}{dX}, \quad \Gamma^1_{11} = \frac{1}{2\varepsilon}\frac{d\ln a}{dX}. \tag{39}$$

Let $u_i(X,x,y)$ be the components of the displacement vector. The extension strains $\gamma_{\alpha\beta}$ and bending strains $\rho_{\alpha\beta}$ are expressed in terms of u_i as follows (Berdichevsky, 2009):

$$2\gamma_{\alpha\beta} = r^i_\alpha\frac{\partial u_i}{\partial x_\beta} + r^i_\beta\frac{\partial u_i}{\partial x_\alpha},$$
$$2\rho_{\alpha\beta} = \frac{\partial}{\partial x_\beta}\left(n_i\frac{\partial u^i}{\partial x_\alpha}\right) + \frac{\partial}{\partial x_\alpha}\left(n_i\frac{\partial u^i}{\partial x_\beta}\right) - 2\Gamma^\gamma_{\alpha\beta}n_i\frac{\partial u^i}{\partial x_\gamma} + \theta\left(e_{\gamma\alpha}b^\gamma_\beta + e_{\gamma\beta}b^\gamma_\alpha\right) \tag{40}$$

where $e_{\alpha\beta}$ denotes surface Levi–Civita tensor ($e_{11} = e_{22} = 0, e_{12} = -e_{21} = \sqrt{a}$). θ is the angle of rotation of the surface elements around the normal vector:

$$\theta = \frac{1}{2\sqrt{a}}\left(r^i_1\frac{\partial u_i}{\partial x_2} - r^i_2\frac{\partial u_i}{\partial x_1}\right) \tag{41}$$

Note that $u^i = u_i$ because u_i are the displacement components in the Cartesian coordinate systems $\hat{\mathbf{e}}_i$. While $\gamma_{\alpha\beta}$ and $\rho_{\alpha\beta}$ are tensor components in surface coordinates, and, therefore the components with upper indices acquire additional metric factors. Because $X = x_1/\varepsilon$, we have

$$\frac{\partial u_i}{\partial x_1} = \frac{\partial u_i}{\partial x} = \frac{\partial u_i}{\partial X}\frac{\partial X}{\partial x}\Big|_{x=\text{const}} + \frac{\partial u_i}{\partial x}\Big|_{X=\text{const}} = \frac{1}{\varepsilon}u'_i + u_{i,1}, \tag{42}$$

with $u'_i = \frac{\partial u_i}{\partial X}|_{x=\text{const}}$ and $u_{i,1} = \frac{\partial u_i}{\partial x}|_{X=\text{const}}$. We also denote $u_{i,2} = \frac{\partial u_i}{\partial x_2} = \frac{\partial u_i}{\partial y}$.

The elastic behavior of the shell is governed by its strain energy density which is given by the following expression:

$$\Phi = \mu h\left(\sigma\left(a^{\alpha\beta}\gamma_{\alpha\beta}\right)^2 + a^{\alpha\beta}a^{\gamma\delta}\gamma_{\alpha\gamma}\gamma_{\beta\delta}\right) + \frac{\mu h^3}{12}\left(\sigma\left(a^{\alpha\beta}\rho_{\alpha\beta}\right)^2 + a^{\alpha\beta}a^{\gamma\delta}\rho_{\alpha\gamma}\rho_{\beta\delta}\right). \tag{43}$$

Here in Eq. (43) $\mu = E/2(1+\nu)$ is the shear modulus, ν the Poisson's ratio, and $\sigma = \nu/(1-\nu)$. The first part is the extension energy and second part the bending energy. The strain energy of the unit cell can be written as

$$J = \langle\Phi\sqrt{a}\rangle = \left\langle \mu h\sqrt{a}\left((1+\sigma)\left(\frac{\gamma_{11}}{a} + \nu\gamma_{22}\right)^2 + \left(\frac{1+2\sigma}{1+\sigma}\right)\gamma^2_{22} + \frac{2}{a}\gamma^2_{12}\right)\right\rangle + \left\langle\frac{\mu h^3}{12}\sqrt{a}\left((1+\sigma)\left(\frac{\rho_{11}}{a} + \nu\rho_{22}\right)^2 + \left(\frac{1+2\sigma}{1+\sigma}\right)\rho^2_{22} + \frac{2}{a}\rho^2_{12}\right)\right\rangle \tag{44}$$

with $\nu = \sigma/(1+\sigma)$. Here the material parameters μ, σ and the shell thickness h could be functions of X, but for simplicity, we assume that they are constant.

4. Asymptotic analysis of the shell strain energy

To model the corrugated structure by an equivalent plate, we start by setting for the shell displacements the presentation following from the general theory of periodic structures (Bakhvalov, 1974; Bakhvalov and Panasenko, 1989):

$$u_\alpha(X,x,y) = v_\alpha(x,y) + \varepsilon\psi_\alpha(X,x,y),$$
$$u_3(X,x,y) = v_3(x,y) + \varepsilon\psi_3(X,x,y). \tag{45}$$

In fact, this is a short cut, and Eq. (45) can be derived by the variational asymptotic method (Berdichevsky, 2009), chapter 17.2. In Eq. (45), v_i have the meaning of the effective plate displacements, and ψ_i are some functions which are periodic in X. Without loss of generality, we can define v_i as the average of u_i over the cell:

$$v_i(x,y) = \langle u_i(X,x,y)\rangle. \tag{46}$$

Then, obviously,

$$\langle\psi_i(X,x,y)\rangle = 0. \tag{47}$$

Substituting Eq. (45) into Eq. (40) and using Eq. (42), we obtain for the strain measures:

$$\gamma_{11} = v_{1,1} + \varphi v_{3,1} + \psi'_1 + \varphi\psi'_3 + \varepsilon(\psi_{1,1} + \varphi\psi_{3,1}),$$
$$2\gamma_{12} = v_{1,2} + v_{2,1} + \varphi v_{3,2} + \psi'_2 + \varepsilon(\psi_{1,2} + \psi_{2,1} + \varphi\psi_{3,2}),$$
$$\gamma_{22} = v_{2,2} + \varepsilon\psi_{2,2},$$
$$\rho_{11} = \frac{1}{\varepsilon}U'_1 - \frac{1}{2\varepsilon}(\ln a)'U_1 + U_{1,1} = \frac{\sqrt{a}}{\varepsilon}\left(\frac{U_1}{\sqrt{a}}\right)' + U_{1,1},$$
$$2\rho_{12} = U_{1,2} + U_{2,1} + \frac{1}{\varepsilon}U'_2 + \frac{\varphi'}{\varepsilon a^{3/2}}\sqrt{a}\theta,$$
$$\rho_{22} = U_{2,2}. \tag{48}$$

Here comma in indices denotes derivatives with respect to x_α, prime the derivative with respect to X. Besides, we introduced the notations,

$$U_1 = n_1(v_{1,1} + \psi'_1) + n_3(\psi'_3 + v_{3,1}) + \varepsilon(n_1\psi_{1,1} + n_3\psi_{3,1}), \tag{49}$$
$$U_2 = n_1 v_{1,2} + n_3 v_{3,2} + \varepsilon(n_1\psi_{1,2} + n_3\psi_{3,2}). \tag{50}$$

Rotation θ can be found from Eq. (41),

$$2\sqrt{a}\theta = v_{1,2} - v_{2,1} + \varphi v_{3,2} - \psi_2' + \varepsilon(\psi_{1,2} - \psi_{2,1} + \varphi\psi_{3,2}).$$

Our objective is to construct an equivalent plate model, i.e. the equations for v_i. To this end, assuming that v_i are known, we seek for the expression of ψ_i in terms of v_i and their derivatives.

4.1. Step 1: discarding doubtful terms

Following the variational asymptotic method, we drop all the terms that are asymptotically small in terms of known small parameters in the energy functional. To model the corrugated structure as a flat plate, we implicitly assume that the corrugated plate is formed by many cells, we have $\varepsilon/L \ll 1$, where L is the characteristic length of macroscopic deformations. Due to the smallness of ε/L, we can drop in the energy the terms associated with derivatives $\psi_{1,1} + \varphi\psi_{3,1}$ in γ_{11}, terms associated with $\psi_{2,1}$ in $2\gamma_{12}$, terms associated with $U_{1,1}$ in ρ_{11}, terms associated with $U_{2,1}$ in $2\rho_{12}$, terms associated with $n_1\psi_{1,1} + n_3\psi_{3,1}$ in U_1, terms associated with $\psi_{2,1}$ in $2\sqrt{a}\theta$, and $U_{2,2}$ in ρ_{22}. However, the terms containing $(\psi_1' + \varphi\psi_3')\psi_{2,2}, \psi_2'(\psi_{1,2} + \varphi\psi_{3,2}), (n_1\psi_{1,2}' + n_3\psi_{3,2}')\psi_2'$ and $(n_1\psi_{1,2} + n_3\psi_{3,2})'\psi_2'$ are doubtful as we do not know the relative orders of ψ_i and there is no clear larger terms than these terms. As suggested in Berdichevsky (2009), we will first discard them and later to check whether they are indeed asymptotically smaller that the terms we keep. The leading terms of the energy in the first approximation are

$$J_0 = \left\langle \mu h\sqrt{a}\left((1+\sigma)\left(\frac{\gamma_{11}^0}{a} + \nu\gamma_{22}^0\right)^2 + \left(\frac{1+2\sigma}{1+\sigma}\right)(\gamma_{22}^0)^2 + \frac{2}{a}(\gamma_{12}^0)^2\right)\right\rangle + \left\langle \frac{\mu h^3}{12}\sqrt{a}\left((1+\sigma)\left(\frac{\rho_{11}^0}{a} + \nu\rho_{22}^0\right)^2 + \left(\frac{1+2\sigma}{1+\sigma}\right)(\rho_{22}^0)^2 + \frac{2}{a}(\rho_{12}^0)^2\right)\right\rangle \tag{51}$$

with

$$\gamma_{11}^0 = v_{1,1} + \varphi v_{3,1} + \psi_1' + \varphi\psi_3', \quad 2\gamma_{12}^0 = v_{1,2} + v_{2,1} + \varphi v_{3,2} + \psi_2',$$
$$\gamma_{22}^0 = v_{2,2}, \quad \rho_{11}^0 = \frac{\sqrt{a}}{\varepsilon}\left(\frac{U_1^0}{\sqrt{a}}\right)', \quad 2\rho_{12}^0 = \frac{1}{\varepsilon}U_2^{0\prime} + \frac{\varphi'}{\varepsilon a^{3/2}}\sqrt{a}\theta^0,$$
$$\rho_{22}^0 = 0. \tag{52}$$

and

$$\begin{aligned} U_1^0 &= n_1(v_{1,1} + \psi_1') + n_3(\psi_3' + v_{3,1}) \\ U_2^0 &= n_1 v_{1,2} + n_3 v_{3,2} \\ 2\sqrt{a}\theta^0 &= v_{1,2} - v_{2,1} + \varphi v_{3,2} - \psi_2' \end{aligned} \tag{53}$$

Substituting Eq. (53) into the bending strains in Eq. (52) and considering

$$n_3 - n_1\varphi = \sqrt{a} \quad n_1' = \frac{-\varphi'}{a^{3/2}} \quad n_3' = \frac{-\varphi\varphi'}{a^{3/2}}. \tag{54}$$

we have

$$\rho_{11}^0 = \frac{\sqrt{a}}{\varepsilon}\left(\psi_3' - \frac{\varphi}{a}\gamma_{11}^0\right)' \quad 2\rho_{12}^0 = -\frac{\varphi'}{2\varepsilon a^{3/2}}(2\gamma_{12}^0) \tag{55}$$

$\gamma_{22}^0, \rho_{22}^0$ do not involve ψ_i, $2\gamma_{12}^0, 2\rho_{12}^0$ involve ψ_2 only, and $\gamma_{11}^0, \rho_{11}^0$ involve ψ_1, ψ_3.

Let us focus on solving ψ_2 first. The strain energy in Eq. (51) related with ψ_2 is:

$$J_2 = \left\langle \mu h\frac{1}{2\sqrt{a}}\left((2\gamma_{12}^0)^2 + \frac{h^2}{12}(2\rho_{12}^0)^2\right)\right\rangle. \tag{56}$$

We need to minimize $2\gamma_{12}^0, 2\rho_{12}^0$ in Eq. (56) over periodic functions $\psi_2(X)$ subject to the constraints Eq. (47). The constraints can be taken care of by introducing the Lagrange multipliers. The corresponding Euler–Lagrange equation is:

$$\left(\frac{1}{\sqrt{a}}\left(2\gamma_{12}^0 - \frac{h^2}{12}2\rho_{12}^0\frac{\varphi'}{2\varepsilon a^{3/2}}\right)\right)' - \lambda_2 = 0. \tag{57}$$

along with boundary conditions

$$[\psi_2] = 0, \quad \left[\frac{1}{\sqrt{a}}\left(2\gamma_{12}^0 - \frac{h^2}{12}2\rho_{12}^0\frac{\varphi'}{2\varepsilon a^{3/2}}\right)\right] = 0. \tag{58}$$

with the square brackets denoting the difference between the end values, for example $[\psi_2] = \psi_2(\frac{1}{2}) - \psi_2(-\frac{1}{2})$. The second condition in Eq. (58) leads to $\lambda_2 = 0$. Hence:

$$\frac{1}{\sqrt{a}}\left(2\gamma_{12}^0 - \frac{h^2}{12}2\rho_{12}^0\frac{\varphi'}{2\varepsilon a^{3/2}}\right) = c_2. \tag{59}$$

Thus:

$$2\gamma_{12}^0 = \frac{\sqrt{a}c_2}{1 + \frac{\varphi'^2h^2}{48\varepsilon^2a^3}}, \tag{60}$$

$$v_{1,2} + v_{2,1} + \varphi v_{3,2} + \psi_2' = \frac{\sqrt{a}c_2}{1 + \frac{\varphi'^2h^2}{48\varepsilon^2a^3}}. \tag{61}$$

Integrating Eq. (61) over the cell length, we obtain the constant c_2:

$$v_{1,2} + v_{2,1} = \left\langle \frac{\sqrt{a}}{1 + \frac{\varphi'^2h^2}{48\varepsilon^2a^3}}\right\rangle c_2, \tag{62}$$

$$c_2 = \alpha_1(v_{1,2} + v_{2,1}). \tag{63}$$

Integrating Eq. (61) with respect to X both sides, we have

$$\psi_2 = -X(v_{1,2} + v_{2,1}) - \phi v_{3,2} + \int_0^X \frac{\sqrt{a}c_2}{1 + \frac{\varphi'^2h^2}{48\varepsilon^2a^3}}dY + const. \tag{64}$$

Considering the constraint in Eq. (47), we can integrate both sides of Eq. (64) over the cell length to solve for the constant, and the final expression for ψ_2 is

$$\psi_2 = -X(v_{1,2} + v_{2,1}) - \phi v_{3,2} + \int_0^X \frac{\sqrt{a}c_2}{1 + \frac{\varphi'^2h^2}{48\varepsilon^2a^3}}dY - \left\langle \int_0^X \frac{\sqrt{a}c_2}{1 + \frac{\varphi'^2h^2}{48\varepsilon^2a^3}}dY\right\rangle. \tag{65}$$

The strain energy in Eq. (51) related with ψ_1 and ψ_3 is:

$$J_1 = \left\langle \mu h\sqrt{a}(1+\sigma)\left(\frac{\gamma_{11}^0}{a} + \nu\gamma_{22}^0\right)^2 + \frac{\mu h^3}{12}\sqrt{a}(1+\sigma)\left(\frac{\rho_{11}^0}{a} + \nu\rho_{22}^0\right)^2\right\rangle. \tag{66}$$

Similarly, we use Lagrange multiplier to take care of the constraints of ψ_1 and ψ_3 in Eq. (47). The corresponding Euler–Lagrange equations are:

$$\begin{aligned} &\left(\frac{1}{\sqrt{a}}\left(\frac{\gamma_{11}^0}{a} + \nu\gamma_{22}^0\right) + \frac{h^2}{12\varepsilon}\left(\frac{\rho_{11}^0}{a} + \nu\rho_{22}^0\right)'\frac{\varphi}{a}\right)' - \lambda_1 = 0, \\ &\left(\frac{\varphi}{\sqrt{a}}\left(\frac{\gamma_{11}^0}{a} + \nu\gamma_{22}^0\right) - \frac{h^2}{12\varepsilon}\left(\frac{\rho_{11}^0}{a} + \nu\rho_{22}^0\right)'\frac{1}{a}\right)' - \lambda_3 = 0. \end{aligned} \tag{67}$$

along with boundary conditions

$$[\psi_1]=0,\quad [\psi_1']=0,\quad \left[\frac{1}{\sqrt{a}}\left(\frac{\gamma_{11}^0}{a}+\nu\gamma_{22}^0\right)+\frac{h^2}{12\varepsilon}\left(\frac{\rho_{11}^0}{a}+\nu\rho_{22}^0\right)'\frac{\varphi}{a}\right]=0,$$
$$[\psi_3]=0,\quad [\psi_3']=0,\quad \left[\frac{\varphi}{\sqrt{a}}\left(\frac{\gamma_{11}^0}{a}+\nu\gamma_{22}^0\right)-\frac{h^2}{12\varepsilon}\left(\frac{\rho_{11}^0}{a}+\nu\rho_{22}^0\right)'\frac{1}{a}\right]=0,$$
$$\left[\frac{\rho_{11}^0}{a}+\nu\rho_{22}^0\right]=0. \tag{68}$$

The third and sixth conditions in Eq. (68) leads to $\lambda_1=\lambda_3=0$. Hence:

$$\frac{1}{\sqrt{a}}\left(\frac{\gamma_{11}^0}{a}+\nu\gamma_{22}^0\right)+\frac{h^2}{12\varepsilon}\left(\frac{\rho_{11}^0}{a}+\nu\rho_{22}^0\right)'\frac{\varphi}{a}=c_1, \tag{69}$$

$$\frac{\varphi}{\sqrt{a}}\left(\frac{\gamma_{11}^0}{a}+\nu\gamma_{22}^0\right)-\frac{h^2}{12\varepsilon}\left(\frac{\rho_{11}^0}{a}+\nu\rho_{22}^0\right)'\frac{1}{a}=c_3. \tag{70}$$

Integrate ($\varphi\times$ (69) − (70)) over the cell length with considering the seventh conditions in Eq. (68) conclude $c_3=0$.

Then Eqs. (69) and (70) can be simplified as:

$$\left(\frac{\rho_{11}^0}{a}+\nu\rho_{22}^0\right)'=c_1\frac{12\varphi\varepsilon}{h^2}, \tag{71}$$

$$\left(\frac{\gamma_{11}^0}{a}+\nu\gamma_{22}^0\right)=\frac{c_1}{\sqrt{a}}. \tag{72}$$

Integrate Eq. (71)

$$\left(\frac{\rho_{11}^0}{a}+\nu\rho_{22}^0\right)=c_1\frac{12x_3}{h^2}+c_4, \tag{73}$$

Rewrite Eq. (73) considering Eq. (55)

$$\left(\psi_3'-\frac{\varphi}{a}\gamma_{11}^0\right)'=\varepsilon\left(c_1\frac{12}{h^2}x_3\sqrt{a}+c_4\sqrt{a}\right). \tag{74}$$

Integrate over the cell length with the fact $[\psi_3'-\frac{\varphi}{a}\gamma_{11}^0]=0, c_4$ is:

$$c_4=-\frac{12}{h^2}c_1\frac{\langle x_3\sqrt{a}\rangle}{\langle\sqrt{a}\rangle}. \tag{75}$$

Integrate Eq. (74) considering c_4,

$$\psi_3'-\frac{\varphi}{a}\gamma_{11}^0=-\frac{12\varepsilon^2}{h^2}c_1\mathcal{A}+c_5. \tag{76}$$

$\varphi\times$ (72) + (76) gives

$$\psi_3'+\nu\varphi\gamma_{22}^0=\frac{c_1\varphi}{\sqrt{a}}-\frac{12\varepsilon^2}{h^2}c_1\mathcal{A}+c_5, \tag{77}$$

Integrating over the cell length, we obtain

$$c_5=-c_1\left\langle\frac{\varphi}{\sqrt{a}}\right\rangle+\frac{12\varepsilon^2}{h^2}c_1\langle\mathcal{A}\rangle. \tag{78}$$

Substitute c_5 into Eq. (77):

$$\psi_3'=-\nu\varphi\gamma_{22}^0+c_1\left(\frac{\varphi}{\sqrt{a}}-\left\langle\frac{\varphi}{\sqrt{a}}\right\rangle\right)-\frac{12\varepsilon^2}{h^2}c_1(\mathcal{A}-\langle\mathcal{A}\rangle). \tag{79}$$

Rewrite Eq. (72) as

$$v_{1,1}+\varphi v_{3,1}+\psi_1'+\varphi\psi_3'=c_1\sqrt{a}-\nu a\gamma_{22}^0, \tag{80}$$

Substituting Eq. (79) into Eq. (80), we have

$$\psi_1'=-(v_{1,1}+\nu v_{2,2}+\varphi v_{3,1})+c_1\left(\frac{1}{\sqrt{a}}+\varphi\left\langle\frac{\varphi}{\sqrt{a}}\right\rangle\right)+\frac{12\varepsilon^2}{h^2}c_1(\varphi\mathcal{A}-\varphi\langle\mathcal{A}\rangle). \tag{81}$$

Integrate over the cell length:

$$v_{1,1}+\nu v_{2,2}=\frac{12\varepsilon^2}{h^2}c_1\langle\varphi\mathcal{A}\rangle+c_1\left\langle\frac{1}{\sqrt{a}}\right\rangle, \tag{82}$$

which can be used to solve for c_1 as

$$c_1=-\frac{(v_{1,1}+\nu v_{2,2})}{\mathcal{C}}. \tag{83}$$

Integrating Eq. (79) both sides with respect to X, we have

$$\psi_3=-\nu\phi\gamma_{22}^0+c_1\left(\int_0^X\frac{\varphi}{\sqrt{a}}dY-X\left\langle\frac{\varphi}{\sqrt{a}}\right\rangle\right)-\frac{12\varepsilon^2}{h^2}c_1\left(\int_0^X\mathcal{A}dY-X\langle\mathcal{A}\rangle\right)+const. \tag{84}$$

Considering the constraint in Eq. (47), we can integrate both sides of Eq. (84) over the cell length to solve for the constant, and the final expression for ψ_3 is

$$\psi_3=-\nu\phi\gamma_{22}^0+c_1\left(\int_0^X\frac{\varphi}{\sqrt{a}}dY-\left\langle\int_0^X\frac{\varphi}{\sqrt{a}}dY\right\rangle-X\left\langle\frac{\varphi}{\sqrt{a}}\right\rangle\right)-\frac{12\varepsilon^2}{h^2}c_1\left(\int_0^X\mathcal{A}dY-\left\langle\int_0^X\mathcal{A}dY\right\rangle-X\langle\mathcal{A}\rangle\right). \tag{85}$$

Integrating Eq. (81) both sides with respect to X, we have

$$\psi_1=-(Xv_{1,1}+\nu Xv_{2,2}+\phi v_{3,1})+c_1\left(\int_0^X\frac{1}{\sqrt{a}}dY+\phi\left\langle\frac{\varphi}{\sqrt{a}}\right\rangle\right)+\frac{12\varepsilon^2}{h^2}c_1\left(\int_0^X\varphi\mathcal{A}dY-\phi\langle\mathcal{A}\rangle\right)+const. \tag{86}$$

Considering the constraint in Eq. (47), we can integrate both sides of Eq. (86) over the cell length to solve for the constant, and the final expression for ψ_1 is

$$\psi_1=-(Xv_{1,1}+\nu Xv_{2,2}+\phi v_{3,1})+c_1\left(\int_0^X\frac{1}{\sqrt{a}}dY-\left\langle\int_0^X\frac{1}{\sqrt{a}}dY\right\rangle+\phi\left\langle\frac{\varphi}{\sqrt{a}}\right\rangle\right)+\frac{12\varepsilon^2}{h^2}c_1\left(\int_0^X\varphi\mathcal{A}dY-\left\langle\int_0^X\varphi\mathcal{A}dY\right\rangle-\phi\langle\mathcal{A}\rangle\right). \tag{87}$$

4.2. Step 2: corrected with doubtful terms

Inspecting Eqs. (65) and (87), we find out that there are $\phi v_{3,\alpha}$ contained in these two functions. This means we cannot drop the aforementioned terms, $(\psi_1'+\varphi\psi_3')\psi_{2,2}, \psi_2'(\psi_{1,2}+\varphi\psi_{3,2})$, $(n_1\psi_{1,2}'+n_3\psi_{3,2}')\psi_2'$, and $(n_1\psi_{1,2}+n_3\psi_{3,2})'\psi_2'$ completely, but should keep the major contributions contained in these terms. In the same way, we also need to recover those terms which are of similar orders into the strain expressions. Thus, for γ_{11}^0, we recover $-x_3v_{3,11}$ from the neglected term $\varepsilon\psi_{1,1}$

$$\gamma_{11}^0=v_{1,1}-x_3v_{3,11}+\varphi v_{3,1}+\psi_1'+\varphi\psi_3'. \tag{88}$$

For $2\gamma_{12}^0$, we recover $-2x_3v_{3,12}$ from the neglected terms $\varepsilon(\psi_{1,2}+\psi_{2,1})$

$$2\gamma_{12}^0=v_{1,2}+v_{2,1}-2x_3v_{3,12}+\varphi v_{3,2}+\psi_2'. \tag{89}$$

For γ_{22}^0, we recover $-x_3v_{3,22}$ from the neglected terms $\varepsilon\psi_{2,2}$

$$\gamma_{22}^0=v_{2,2}-x_3v_{3,22}. \tag{90}$$

For ρ_{11}^0, we recover $(n_3-n_1\varphi)v_{3,11}=\sqrt{a}v_{3,11}$ from the neglected term $U_{1,1}$

$$\rho_{11}^0=\frac{\sqrt{a}}{\varepsilon}\left(\frac{U_1^0}{\sqrt{a}}\right)'+\sqrt{a}v_{3,11}. \tag{91}$$

For $2\rho_{12}^0$, we recover $(\sqrt{a}+n_3)v_{3,12}$ from the neglected terms in $U_{1,2}+U_{2,1}$

$$2\rho_{12}^0 = (\sqrt{a}+n_3)v_{3,12} + \frac{1}{\varepsilon}U_2^{0\prime} + \frac{\varphi'}{\varepsilon a^{3/2}}\sqrt{a}\theta^0. \tag{92}$$

For ρ_{22}^0, we recover $n_3 v_{3,12}$ from the neglected terms in $U_{2,2}$

$$\rho_{22}^0 = n_3 v_{3,22}. \tag{93}$$

For U_1^0, we recover $-x_3 v_{3,11}$ from the neglected term $\varepsilon\psi_{1,1}$

$$U_1^0 = n_1(v_{1,1} - x_3 v_{3,11} + \psi_1') + n_3(\psi_3' + v_{3,1}). \tag{94}$$

For U_2^0, we recover $-x_3 v_{3,12}$ from the neglected term $\varepsilon\psi_{1,2}$

$$U_2^0 = n_1(v_{1,2} - x_3 v_{3,12}) + n_3 v_{3,2}. \tag{95}$$

For θ^0, the major terms contributed from the neglected term $\varepsilon(\psi_{1,2}-\psi_{2,1})$ cancel each other, so that

$$2\sqrt{a}\theta^0 = v_{1,2} - v_{2,1} + \varphi v_{3,2} - \psi_2'. \tag{96}$$

Using Eqs. (94)–(96), we can rewrite the bending strains as

$$\begin{aligned}
\rho_{11}^0 &= \frac{\sqrt{a}}{\varepsilon}\left(\psi_3' - \frac{\varphi}{a}\gamma_{11}^0\right)' + \sqrt{a}v_{3,11},\\
2\rho_{12}^0 &= 2\sqrt{a}v_{3,12} - \frac{\varphi'}{2\varepsilon a^{3/2}}(2\gamma_{12}^0),\\
\rho_{22}^0 &= \frac{1}{\sqrt{a}}v_{3,22}.
\end{aligned} \tag{97}$$

Substituting this new set of strain measures into Eq. (51), we need to carry out the solution procedure again. Most of the equations starting Eq. (56) to Eq. (87) remain the same, except the changes listed in the Appendix.

5. Equivalent plate energy

Now, everything is ready to compute the equivalent plate energy. It is convenient to split the first approximation of the strain energy in Eq. (51) into three parts. J_1 is associated with energy in Eq. (66), J_2 with energy in Eq. (56), and J_3 with energy

$$J_3 = \left\langle \mu h\sqrt{a}(1+\nu)(\gamma_{22}^0)^2 + \frac{\mu h^3}{12}\sqrt{a}(1+\nu)(\rho_{22}^0)^2 \right\rangle. \tag{98}$$

Let us compute J_1 first. Using Eq. (72) and Eq. (73)

$$J_1 = \left\langle \mu h\sqrt{a}(1+\sigma)\left(\frac{c_1}{\sqrt{a}}\right)^2 + \frac{\mu h^3}{12}\sqrt{a}(1+\sigma)\left(c_1\frac{12x_3}{h^2}+c_4\right)^2 \right\rangle. \tag{99}$$

Substituting Eq. (17) and Eq. (15) into Eq. (99), J_1 becomes,

$$\begin{aligned}
J_1 = {} & (v_{1,1}+\nu v_{2,2})^2\mu(1+\sigma)\frac{1}{\mathcal{C}^2}\left(h\left\langle\frac{1}{\sqrt{a}}\right\rangle + \frac{12}{h}\varepsilon^2\langle\varphi\mathcal{A}\rangle\right)\\
& + (v_{3,11}+\nu v_{3,22})^2\mu h(1+\sigma)\left(\frac{\varepsilon^2\mathcal{B}^2}{\mathcal{C}^2}\left\langle\frac{1}{\sqrt{a}}\right\rangle + \frac{h^2}{12}\left(\frac{12^2\varepsilon^4\mathcal{B}^2}{h^4\mathcal{C}^2}\langle\varphi\mathcal{A}\rangle + \frac{1}{\langle\sqrt{a}\rangle}\right)\right)\\
& - (v_{1,1}+\nu v_{2,2})(v_{3,11}+\nu v_{3,22})\mu h(1+\sigma)\left(\frac{2\varepsilon\mathcal{B}}{\mathcal{C}^2}\left\langle\frac{1}{\sqrt{a}}\right\rangle + \frac{24\mathcal{B}\varepsilon^3}{h^2\mathcal{C}^2}\langle\varphi\mathcal{A}\rangle\right).
\end{aligned} \tag{100}$$

Note

$$\langle\sqrt{a}(x_3-\mathcal{B}\varepsilon)^2\rangle = \langle\sqrt{a}x_3^2\rangle - \frac{\langle\sqrt{a}x_3\rangle^2}{\langle\sqrt{a}\rangle} = \varepsilon^2\langle\varphi\mathcal{A}\rangle, \quad \frac{\langle\sqrt{a}(x_3-\varepsilon\mathcal{B})\rangle}{\langle\sqrt{a}\rangle} = 0.$$

Rewriting Eq. (56)

$$J_2 = \frac{\mu h}{2}\left\langle\frac{1}{\sqrt{a}}\left((2\gamma_{12}^0)^2 + \frac{h^2}{12}\left(2\sqrt{a}v_{3,12} - \frac{\varphi'}{2\varepsilon a^{3/2}}2\gamma_{12}^0\right)^2\right)\right\rangle. \tag{101}$$

Substituting Eq. (107) and Eq. (16) into Eq. (101),

$$\begin{aligned}
J_2 = {} & (v_{1,2}+v_{2,1})^2\left(\frac{\mu h\alpha_1^2}{2}\left\langle\frac{\sqrt{a}}{(1+\frac{\varphi'^2h^2}{48\varepsilon^2a^3})}\right\rangle\right)\\
& + v_{3,12}^2\frac{\mu h}{2}\left\langle\frac{\sqrt{a}h^2}{3} - \frac{1}{\sqrt{a}}\frac{\frac{h^4\varphi'^2}{12^2\varepsilon^2a^2} - a\alpha_2^2}{1+\frac{\varphi'^2h^2}{48\varepsilon^2a^3}}\right\rangle\\
& - (v_{1,2}+v_{2,1})v_{3,12}\mu h\alpha_1\alpha_2\left\langle\frac{\sqrt{a}}{1+\frac{\varphi'^2h^2}{48\varepsilon^2a^3}}\right\rangle.
\end{aligned} \tag{102}$$

Substituting γ_{22}^0 in Eq. (90) and ρ_{22}^0 in Eq. (97) into Eq. (98),

$$\begin{aligned}
J_3 = {} & v_{2,2}^2\mu h(1+\nu)\langle\sqrt{a}\rangle + v_{3,22}^2\mu h(1+\nu)\left(\langle\sqrt{a}x_3^2\rangle + \frac{h^2}{12}\left\langle\frac{1}{\sqrt{a}}\right\rangle\right)\\
& - v_{2,2}v_{3,22}2\mu h(1+\nu)\langle\sqrt{a}x_3\rangle.
\end{aligned} \tag{103}$$

If we set

$$\begin{aligned}
&\epsilon_{xx} = v_{1,1}, \quad \epsilon_{yy} = v_{2,2}, \quad 2\epsilon_{xy} = v_{1,2}+v_{2,1},\\
&\kappa_{xx} = -v_{3,11}, \quad \kappa_{yy} = -v_{3,22}, \quad \kappa_{xy} = -v_{3,12},
\end{aligned} \tag{104}$$

we obtain the strain energy in Eq. (1) with the equivalent plate stiffnesses listed in Eq. (11).

6. Recovery relations

The equivalent plate stiffnesses constants can be used as inputs to carry out a plate analysis, either analytically or numerically, to predict the plate displacement field (v_i) and strain field ($\epsilon_{xx}, \epsilon_{yy}, 2\epsilon_{xy}, \kappa_{xx}, \kappa_{yy}, 2\kappa_{xy}$). This information can be used first to recover displacement field in the original corrugated shell using Eq. (45) with ψ_i solved previously in Eq. (124), (111), and (122). Usually it is more critical to know the strain field within the original corrugated shell as those given in Eq. (14). The stress resultants can be recovered using the constitutive relation corresponding to the strain energy in Eq. (44), which can be used to further recover the three-dimensional (3D) stresses based on the relations of the starting shell theory and the three-dimensional elasticity theory.

7. Some examples

In this section, two shapes of corrugations are studied. One is a sinusoidal corrugation which represents the symmetric case with no coupling effects, and the other is a exponential–sinusoidal corrugation which is an example of the nonsymmetric corrugations thus exhibiting coupling effects.

7.1. Sinusoidal shape

The mid-surface of sinusoidal shape,

$$\phi(X) = \frac{T}{\varepsilon}\sin(2\pi X). \tag{105}$$

is characterized by one parameter, T, the rise of the corrugation Fig. 3. For numerical values we choose $\varepsilon = 0.64$ m, $T = 0.11$ m, $h = 0.005$ m and material properties are taken to be $E = 30$GPa, $\nu = 0.2$, $\rho = 7830$ kg/m^3. The equivalent plate stiffnesses obtained using different approaches are listed in Table 1. VAPAS is a code introduced in Lee and Yu (2011) for equivalent plate modeling of panels with microstructures starting from the original 3D elasticity theory. Corrugated structures can be considered as a special case of such panels and the results obtained can be used as benchmark for the present study. For the corrugated profile under consideration, $\langle\phi\sqrt{a}\rangle = 0$, and there is no extension–bending coupling. It is seen from Table 1 that the results obtained by the present

Table 1
Equivalent plate stiffnesses of sinusoidal corrugation.

	Eqs. (5), (8)	Xia et al. (2012)	VAPAS	Present
A_{11} (N/m)	53805	47613	48152	47613
A_{12} (N/m)	10761	9523	9630	9523
A_{22} (N/m)	1.8708×10^8	1.8708×10^8	1.8692×10^8	1.8708×10^8
A_{66} (N/m)	5.0113×10^7	5.0113×10^7	5.0097×10^7	5.0113×10^7
D_{11} (N · m)	261.004	261.004	263.972	261.004
D_{12} (N · m)	52.20	52.20	52.95	52.20
D_{22} (N · m)	1025270	1068260	1022874	1025540
D_{66} (N · m)	162.39	162.39	163.38	162.39

approach are very close to those predicted by VAPAS and Xia et al. However, the differences between the present approach and the commonly accepted formulas for A_{11}, A_{12} are noticeable. Note, in this table, we used $D_{12} = \nu D_{11}$ from Eq. (6). Formula (9) gives $A_{11} = 39639$ N/m, which is also well off the correct result.

We analyzed a square sinusoidal corrugated plate with 11 corrugations subjected to a uniformly distributed pressure using equivalent plate analysis based on the present theory. The results agree with those of a direct finite element analysis using ANSYS with shell elements, as expected. This comparison can be found in reference Ye (2013).

7.2. Exponential–sinusoidal shape

In the second example, a non-symmetric corrugated shape is chosen to show the coupling effects. We use an exponential–sinusoidal function with unit cell length $\varepsilon = 1$ m,

$$\phi(X) = \eta\left(e^{Sin(2\pi X)} - \langle e^{Sin(2\pi X)}\rangle\right), \tag{106}$$

as sketched in Fig. 4. A plot of the dimensionless parameter $B_{22}/(Eh\varepsilon)$ as a function of η is shown in Fig. 5. We choose thickness $h = 0.005$ m and material properties $E = 30$ GPa, $\nu = 0.2$. Equivalent plate stiffnesses obtained by different approaches are listed for

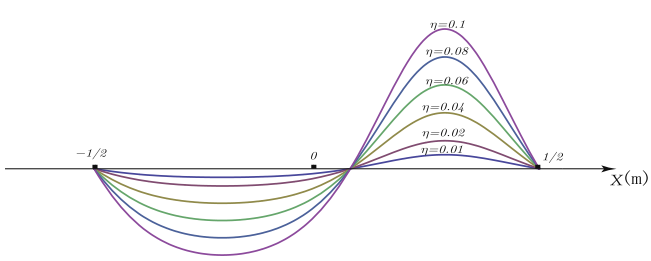

Fig. 4. Shapes of nonsymmetric corrugations for different values of parameter η.

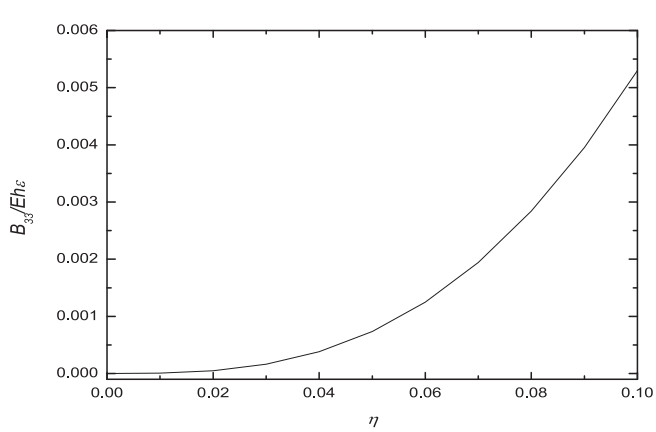

Fig. 5. Coupling coefficient $B_{22}/(Eh\varepsilon)$ as a function of η.

Table 2
Equivalent plate stiffnesses of exponential–sinusoidal corrugation ($\eta = 0.1$).

	Eqs. (5), (8)	Xia et al. (2012)	VAPAS	Present
A_{11} (N/m)	47139	43765	46366	43911
A_{12} (N/m)	9427.89	8753.09	9273.22	8782.20
A_{22}(N/m)	1.6759×10^8	1.7088×10^8	1.7072×10^8	1.7088×10^8
A_{66} (N/m)	5.5942×10^7	5.4865×10^7	5.4846×10^7	5.4866×10^7
B_{11} (N)	N/A	N/A	225.98	204.26
B_{12} (N)	N/A	N/A	42.644	40.851
B_{22} (N)	N/A	N/A	817802	794841
D_{11} (N · m)	291.364	285.757	296.106	286.707
D_{12} (N · m)	58.273	57.151	59.679	57.341
D_{22} (N · m)	1.3297×10^6	1.1622×10^6	1.1122×10^6	1.1157×10^6
D_{66} (N · m)	145.47	148.33	153.29	148.33

comparison in Table 2. Since the corrugation is not symmetric, the rise of the corrugation T in Eq. (8) is measured as half of the total swing. Apparently, the extension–bending coupling, particularly the coupling coefficient B_{22} between $v_{2,2}$ and $v_{3,22}$, is not negligible comparing to other stiffnesses terms as η grows larger. For the other stiffness constants, the four sets of results also have noticeable differences for which the present approach and Xia et al. have a better agreement with VAPAS than the results in Eqs. (5), (8) except A_{11} and A_{12}.

8. Conclusion

The variational asymptotic method has been used to construct an equivalent plate model for corrugated structures. The theory handles general corrugation shape providing the original structure can be described using the classical shell theory and the length of a single corrugation is small with respect to the characteristic length of macroscopic deformation of the corrugated structure. The present theory not only provides a complete set of effective plate stiffnesses but also the complete set of recovery relations to obtain the local fields within the corrugated shell.

Acknowledgment

This work is partially supported by the Liebherr-Aerospace company.

Appendix A. Appendix: changes due to doubtful terms

Eq. (60) is replaced with

$$2\gamma_{12}^0 = \frac{\sqrt{a}c_2 + \frac{h^2\varphi' v_{3,12}}{12\varepsilon a}}{1 + \frac{\varphi'^2 h^2}{48\varepsilon^2 a^3}}. \tag{107}$$

Eq. (61) is replaced with

$$v_{1,2} + v_{2,1} - 2x_3 v_{3,12} + \varphi v_{3,2} + \psi_2' = \frac{\sqrt{a}c_2 + \frac{h^2\varphi' v_{3,12}}{12\varepsilon a}}{1 + \frac{\varphi'^2 h^2}{48\varepsilon^2 a^3}}. \tag{108}$$

Eq. (62) is replaced with

$$v_{1,2} + v_{2,1} = \left\langle \frac{\sqrt{a}}{1 + \frac{\varphi'^2 h^2}{48\varepsilon^2 a^3}} \right\rangle c_2 + \left\langle \frac{\frac{h^2\varphi'}{12\varepsilon a}}{1 + \frac{\varphi'^2 h^2}{48\varepsilon^2 a^3}} \right\rangle v_{3,12}, \tag{109}$$

with c_2 defined in Eq. (16).

Eq. (64) should be replaced with

$$\psi_2 = -X(v_{1,2} + v_{2,1}) - \phi v_{3,2} + 2\int_0^X x_3 dY v_{3,12} + \int_0^X \frac{\sqrt{a}c_2 + \frac{h^2\varphi' v_{3,12}}{12\varepsilon a}}{1 + \frac{\varphi'^2 h^2}{48\varepsilon^2 a^3}} dY + const. \tag{110}$$

Eq. (65) should be replaced with

$$\psi_2 = -X(v_{1,2}+v_{2,1}) - \phi v_{3,2} + 2\left(\int_0^X x_3 dY - \left\langle \int_0^X x_3 dY \right\rangle\right) v_{3,12} + \int_0^X \frac{\sqrt{a}c_2 + \frac{h^2\varphi' v_{3,12}}{12\varepsilon a}}{1+\frac{\varphi'^2 h^2}{48\varepsilon^2 a^3}} dY - \left\langle \int_0^X \frac{\sqrt{a}c_2 + \frac{h^2\varphi' v_{3,12}}{12\varepsilon a}}{1+\frac{\varphi'^2 h^2}{48\varepsilon^2 a^3}} dY \right\rangle. \quad (111)$$

Eq. (74) should be replaced with

$$\left(\psi_3' - \frac{\varphi}{a}\gamma_{11}^0\right)' = \varepsilon\left(c_1 \frac{12}{h^2} x_3\sqrt{a} + c_4\sqrt{a} - (v_{3,11} + v v_{3,22})\right). \quad (112)$$

with c_4 defined in Eq. (17).

Eq. (76) should be replaced with

$$\psi_3' - \frac{\varphi}{a}\gamma_{11}^0 = -\frac{12\varepsilon^2}{h^2} c_1 \mathcal{A} + \varepsilon\left(\frac{\int_0^X \sqrt{a} dY}{\langle\sqrt{a}\rangle} - X\right)(v_{3,11} + v v_{3,22}) + c_5. \quad (113)$$

Eq. (77) should be replaced with

$$\psi_3' + v\varphi\gamma_{22}^0 = \frac{c_1\varphi}{\sqrt{a}} - \frac{12\varepsilon^2}{h^2} c_1 \mathcal{A} + \varepsilon\left(\frac{\int_0^X \sqrt{a} dY}{\langle\sqrt{a}\rangle} - X\right)(v_{3,11} + v v_{3,22}) + c_5. \quad (114)$$

Eq. (78) should be replaced with

$$c_5 = -c_1\left\langle\frac{\varphi}{\sqrt{a}}\right\rangle + \frac{12\varepsilon^2}{h^2} c_1\langle\mathcal{A}\rangle - \varepsilon\frac{\left\langle\int_0^X \sqrt{a} dY\right\rangle}{\langle\sqrt{a}\rangle}(v_{3,11} + v v_{3,22}). \quad (115)$$

Here, notice $\langle\varphi x_3\rangle = 0$.

Eq. (79) should be replaced with

$$\psi_3' = -v\varphi\gamma_{22}^0 + c_1\left(\frac{\varphi}{\sqrt{a}} - \left\langle\frac{\varphi}{\sqrt{a}}\right\rangle\right) - \frac{12\varepsilon^2}{h^2} c_1(\mathcal{A} - \langle\mathcal{A}\rangle) + \varepsilon\left(\frac{\int_0^X \sqrt{a} dY - \left\langle\int_0^X \sqrt{a} dY\right\rangle}{\langle\sqrt{a}\rangle} - X\right)(v_{3,11} + v v_{3,22}). \quad (116)$$

Eq. (80) should be replaced with

$$v_{1,1} - x_3 v_{3,11} + \varphi v_{3,1} + \psi_1' + \varphi\psi_3' = c_1\sqrt{a} - v a\gamma_{22}^0. \quad (117)$$

Eq. (81) should be replaced with

$$\psi_1' = -(v_{1,1} + v v_{2,2} + \varphi v_{3,1}) + x_3(v_{3,11} + v v_{3,22}) + c_1\left(\frac{1}{\sqrt{a}} + \varphi\left\langle\frac{\varphi}{\sqrt{a}}\right\rangle\right) + \frac{12\varepsilon^2}{h^2} c_1(\varphi\mathcal{A} - \varphi\langle\mathcal{A}\rangle) - \varepsilon\left(\frac{\varphi\int_0^X \sqrt{a} dY - \varphi\left\langle\int_0^X \sqrt{a} dY\right\rangle}{\langle\sqrt{a}\rangle} - \varphi X\right)(v_{3,11} + v v_{3,22}). \quad (118)$$

Eq. (82) should be replaced with

$$v_{1,1} + v v_{2,2} = \frac{12\varepsilon^2}{h^2} c_1\langle\varphi\mathcal{A}\rangle + \varepsilon\mathcal{B}(v_{3,11} + v v_{3,22}) + c_1\left\langle\frac{1}{\sqrt{a}}\right\rangle. \quad (119)$$

with the constant $\mathcal{B}$

$$\mathcal{B} = \left(\langle\varphi X\rangle - \frac{\left\langle\varphi\int_0^X \sqrt{a} dY\right\rangle}{\langle\sqrt{a}\rangle}\right) = \frac{\langle\sqrt{a}\rangle\int_{-\frac{1}{2}}^{\frac{1}{2}} X d\phi - \int_{-\frac{1}{2}}^{\frac{1}{2}}\int_0^X \sqrt{a} dY d\phi}{\langle\sqrt{a}\rangle} = \frac{\langle\sqrt{a}\rangle\left(X\phi\big|_{-\frac{1}{2}}^{\frac{1}{2}} - \langle\phi\rangle\right) - \int_0^X \sqrt{a} dY \phi\big|_{-\frac{1}{2}}^{\frac{1}{2}} + \langle\sqrt{a}\phi\rangle}{\langle\sqrt{a}\rangle} = \frac{\langle\sqrt{a}\phi\rangle}{\langle\sqrt{a}\rangle}. \quad (120)$$

Eq. (83) should be replaced with the definition in Eq. (15).

Eq. (84) should be replaced with

$$\psi_3 = -v\phi v_{2,2} + v\int_0^X \varphi x_3 dY v_{3,22} + c_1\left(\int_0^X \frac{\varphi}{\sqrt{a}} dY - X\left\langle\frac{\varphi}{\sqrt{a}}\right\rangle\right) - \frac{12\varepsilon^2}{h^2} c_1\left(\int_0^X \mathcal{A} dY - X\langle\mathcal{A}\rangle\right) + const + \varepsilon\left(\frac{\int_0^X\int_0^Y \sqrt{a} dZ dY - X\left\langle\int_0^X \sqrt{a} dY\right\rangle}{\langle\sqrt{a}\rangle} - \frac{X^2}{2}\right)(v_{3,11} + v v_{3,22}). \quad (121)$$

Eq. (85) should be replaced with

$$\psi_3 = -v\phi v_{2,2} + v\left(\int_0^X \varphi x_3 dY - \left\langle\int_0^X \varphi x_3 dY\right\rangle\right) v_{3,22} + c_1\left(\int_0^X \frac{\varphi}{\sqrt{a}} dY - \left\langle\int_0^X \frac{\varphi}{\sqrt{a}} dY\right\rangle - X\left\langle\frac{\varphi}{\sqrt{a}}\right\rangle\right) - \frac{12\varepsilon^2}{h^2} c_1\left(\int_0^X \mathcal{A} dY - \left\langle\int_0^X \mathcal{A} dY\right\rangle - X\langle\mathcal{A}\rangle\right) + \varepsilon\left(\frac{\int_0^X\int_0^Y \sqrt{a} dZ dY - \left\langle\int_0^X\int_0^Y \sqrt{a} dZ dY\right\rangle - X\left\langle\int_0^X \sqrt{a} dY\right\rangle}{\langle\sqrt{a}\rangle} - \frac{X^2}{2} + \frac{1}{24}\right) \times (v_{3,11} + v v_{3,22}). \quad (122)$$

Eq. (86) should be replaced with

$$\psi_1 = -(X v_{1,1} + v X v_{2,2} + \phi v_{3,1}) + \int_0^X x_3 dY (v_{3,11} + v v_{3,22}) + c_1\left(\int_0^X \frac{1}{\sqrt{a}} dY + \phi\left\langle\frac{\varphi}{\sqrt{a}}\right\rangle\right) + \frac{12\varepsilon^2}{h^2} c_1\left(\int_0^X \varphi\mathcal{A} dY - \phi\langle\mathcal{A}\rangle\right) + const - \varepsilon\left(\frac{\int_0^X \varphi\int_0^Y \sqrt{a} dZ dY - \phi\langle\int_0^X \sqrt{a} dY\rangle}{\langle\sqrt{a}\rangle} - \int_0^X \varphi X dY\right)(v_{3,11} + v v_{3,22}). \quad (123)$$

Eq. (87) should be replaced with

$$\psi_1 = -(X v_{1,1} + v X v_{2,2} + \phi v_{3,1}) + \left(\int_0^X x_3 dY - \left\langle\int_0^X x_3 dY\right\rangle\right)(v_{3,11} + v v_{3,22}) + c_1\left(\int_0^X \frac{1}{\sqrt{a}} dY - \left\langle\int_0^X \frac{1}{\sqrt{a}} dY\right\rangle + \phi\left\langle\frac{\varphi}{\sqrt{a}}\right\rangle\right) + \frac{12\varepsilon^2}{h^2} c_1\left(\int_0^X \varphi\mathcal{A} dY - \left\langle\int_0^X \varphi\mathcal{A} dY\right\rangle - \phi\langle\mathcal{A}\rangle\right) - \varepsilon\left(\frac{\int_0^X \varphi\int_0^Y \sqrt{a} dZ dY - \left\langle\int_0^X \varphi\int_0^Y \sqrt{a} dZ dY\right\rangle - \phi\left\langle\int_0^X \sqrt{a} dY\right\rangle}{\langle\sqrt{a}\rangle} - \int_0^X \varphi X dY + \left\langle\int_0^X \varphi X dY\right\rangle\right)(v_{3,11} + v v_{3,22}). \quad (124)$$

References

Abdel-Sayed, G., 1970. Critical shear loading of curved panels of corrugated sheets. J. Eng. Mech. Div. 96, 895–912.

Aboura, Z., Talbi, N., Allaoui, S., Benzeggagh, M.L., 2004. Elastic behavior of corrugated cardboard: experiments and modeling. Compos. Struct. 63, 53–62.

Andreeva, L.E., 1966. Elastic Elements of Instruments. Israel Program for Scientific Translations.

Andrianov, I.V., Diskovsky, A.A., Kholod, E.G., 1998. Homogenization method in the theory of corrugated plates. Tech. Mech. 18, 123–133.

Andrianov, I.V., Awrejcewicz, J., Diskovsky, A.A., 2009. Asymptotic investigation of corrugated elements with quasi-periodic structures. In: Dynamical Systems – Theory and Applications, vol. 12. Lodz, Poland.
Arkhangelskii, A.F., Gorbachev, V.I., 2007. Effective characteristics of corrugated plates. Mech. Solids 42, 447–462.
Bakhvalov, N.S., 1974. Average characteristics of bodies with periodic structure. Sov. Math. 218, 1046–1048.
Bakhvalov, N.S., Panasenko, G., 1989. Homogenisation: Averaging Processes in Periodic Media. Kluwer-Academic Publishers Group, Norwell, MA/Dordrecht.
Bartolozzi, G., Pierini, M., Orrenius, U., Baldanzini, N., 2013. An equivalent material formulation for sinusoidal corrugated cores of structural sandwich panels. Compos. Struct. 100, 173–185.
Baum, G.A., Brennan, D.C., Habeger, C.C., 1981. Orthotropic elastic constants of paper. Tappi J. 64, 97–101.
Berdichevsky, V.L., 2009. Variational Principles of Continuum Mechanics: II Applications. Springer Verlag.
Briassoulis, D., 1986. Equivalent orthotropic properties of corrugated sheets. Comput. Struct. 23, 129–138.
Buannic, N., Cartraud, P., Quesnel, T., 2003. Homogenization of corrugated core sandwich panels. Compos. Struct. 59, 299–312.
Carlsson, L.A., Nordstrand, T., Westerlind, B., 2001. On the elastic stiffnesses of corrugated core sandwich. J. Sandwich Struct. Mater. 3, 253–267.
Davalos, J.F., Qiao, P.Z., Xu, X.F., Robinson, J., Barth, K.E., 2001. Modeling and characterization of fiber-reinforced plastic honeycomb sandwich panels for highway bridge applications. Compos. Struct. 52, 441–452.
Davies, J.M., 1976. Calculation of steel diaphragm behavior. J. Struct. Div. 102, 1411–1430.
Easley, J.T., 1975. Buckling formulas for corrugated metal shear diaphragms. J. Struct. Div. 101, 1403–1417.
Easley, J.T., McFarland, E.D., 1969. Buckling of light gage corrugated metal shear diaphragms. J. Struct. Div. 95, 1497–1516.
El-Atrouzy, M.N., 1969. Structural properties of corrugated sheets used in cylindrical shells (Master's thesis). The University of Windsor.
El-Atrouzy, M.N., Abdel-Sayed, G., 1978. Prebuckling analysis of orthotropic barrel-shells. J. Struct. Div. 104, 1775–1786.
Gentilinia, C., Nobilea, L., Seffen, K.A., 2009. Numerical analysis of morphing corrugated plates. Procedia Eng. 1, 79–82.
Haj-Ali, R., Choi, J., Wei, B.S., Popil, R., Schaepe, M., 2009. Refined nonlinear finite element models for corrugated fiberboards. Compos. Struct. 87, 321–333.
Huber, M.T., 1923. Die theorie des kreuzweise bewehrten eisenbetonplatten. Der Bauingenieur 4, 354–360.
Lau, J.H., 1981. Stiffness of corrugated plate. J. Eng. Mech. Div. 107, 271–275.
Lee, C.H., 1981. Study of corrugated plates (PhD thesis). University of South Carolina.
Lee, C.Y., Yu, W., 2011. Homogenization and dimensional reduction of composite plates with in-plane heterogeneity. Int. J. Solids Struct. 48, 1474–1484.
Lekhnitskii, S.G., 1968. Anisotropic plates. Technical report, DTIC Document.
Liang, C.C., Yang, M.F., Wu, P.W., 2001. Optimum design of metallic corrugated core sandwich panels subjected to blast loads. Ocean Eng. 28, 825–861.
Liew, K.M., Peng, L.X., Kitipornchai, S., 2006. Buckling analysis of corrugated plates using a mesh-free galerkin method based on the first-order shear deformation theory. Comput. Mech. 38, 61–75.
Liew, K.M., Peng, L.X., Kitipornchai, S., 2009. Vibration analysis of corrugated reissner-mindlin plates using a mesh-free galerkin method. Int. J. Mech. Sci. 51, 642–652.
Luo, S., Suhling, J.C., 1992. The bending stiffnesses of corrugated board. Mech. Cellulosic Mater. 145, 15–26.
Manevich, L.I., Andrianov, I.V., Oshmyan, V.G., 2002. Mechanics of Periodically Heterogeneous Structures. Springer Verlag.
Marzouk, O.A., Abdel-Sayed, G., 1973. Linear theory of orthotropic cylindrical shells. J. Struct. Div. 99, 2287–2306.
Mccready, D.W., Katz, D.L., 1939. A study of corrugated fiberboard the effect of adhesive on the strength of corrugated board. Technical report, Department of Engineering, University of Michigan Ann Arbor.
McFarland, D.E., Smith, B.L., Bernhart, W.D., 1972. Analysis of Plates. Spartan Books.
Samanta, A., Mukhopadhyay, M., 1999. Finite element static and dynamic analyses of folded plates. Eng. Struct. 21, 277–287.
Seaquist Jr., E.O., 1964. Bending of rectangular corrugated sandwich plates (PhD thesis). Iowa State University of Science and Technology.
Seydel, E., 1931. Shear buckling of corrugated plates. Jahrbuch die Deutschen Versuchsanstalt fur Luftfahrt 9, 233–245.
Szilard, R., 1974. Theory and Analysis of Plates. Prentice-Hall.
Talbi, N., Batti, A., Ayad, R., Guo, Y.Q., 2009. An analytical homogenization model for finite element modelling of corrugated cardboard. Compos. Struct. 88, 280–289.
Thill, C., Etches, J.A., Bond, I.P., Potter, K.D., Weaver, P.M., 2010. Composite corrugated structures for morphing wing skin applications. Smart Mater. Struct. 19, 124009.
Troitsky, M.S., 1976. Stiffened Plates: Bending, Stability, and Vibrations. Elsevier.
Viguié, J., Dumont, P.J., Orgéas, L., Vacher, P., Desloges, I., Mauret, E., 2011. Surface stress and strain fields on compressed panels of corrugated board boxes. an experimental analysis by using digital image stereocorrelation. Compos. Struct. 93, 2861–2873.
Wennberg, D., Wennhage, P., Stichel, S., 2011. Orthotropic models of corrugated sheets in finite element analysis. ISRN Mech. Eng. 2011.
Xia, Y., Friswell, M.I., Saavedra Flores, E.I., 2012. Equivalent models of corrugated panels. Int. J. Solids Struct. 49 (13), 1453–1462.
Ye, Z., 2013. Enhance Variational Asymptotic Method for Unit Cell Homogenization (VAMUCH) for Real Engi-neering Structures and Material (PhD thesis). Utah State University.
Yokozeki, T., Takeda, S., Ogasawara, T., Ishikawa, T., 2006. Mechanical properties of corrugated composites for candidate materials of flexible wing structures. Composites Part A 37, 1578–1586.